

Novel imaging phenotypes of naïve asthma patients with distinctive clinical characteristics and T2 inflammation traits

Zhenyu Yang*, Lu Qin* , Jinhan Qiao, Chongsheng Cheng, Yiwen Liu, Shengding Zhang, Xiaoyu Fang, Zhen Li, Harald Renz, Xiansheng Liu, Liming Xia, Qiongjie Hu  and Min Xie 

Abstract

Objective: This study aims to describe the imaging features of naïve asthma patients, defined as not receiving corticosteroids or other asthma medications for at least 1 month, and their association with therapeutic response, and to discover novel unbiased imaging phenotypes. **Methods:** A total of 109 naïve asthma patients and 50 healthy controls were enrolled in this study. Clinical data and imaging indices of high-resolution computed tomography were collected. The correlation between imaging indices and clinical features was analyzed. Cluster analyses were adopted to determine three novel imaging phenotypes. **Results:** Compared with healthy controls, naïve asthma patients presented higher scores of airway remodeling, bronchiectasis, and mucus plugs. Mean airway wall area (WA)% was inversely correlated with mid-expiratory flow velocity% predicted. The extent score of bronchiectasis was positively correlated with smoking history and significantly increased in the high mucus group. Mucus plugs were related to improving lung function and type 2 (T2) inflammation, as assessed by sputum and blood eosinophils and fraction of exhaled nitric oxide. Cluster 1 patients had a high proportion of emphysema, the best lung function, and the lowest T2 inflammation; cluster 2 patients had severe airway remodeling, relatively good lung function, and moderate T2 inflammation; cluster 3 patients had severe airway remodeling, mucus plugs, and bronchiectasis, and showed the worst lung function and highest T2 inflammation. **Conclusion:** Naïve asthma patients had the imaging traits of airway remodeling, bronchiectasis, and mucus plugs. The unbiased imaging phenotypes had good consistency with clinical characteristics, therapeutic response, and T2 inflammation expression in naïve asthma patients.

Keywords: asthma, cluster analysis, phenotype, X-ray computed tomography

Received: 28 June 2021; revised manuscript accepted: 14 February 2022.

Introduction

Asthma is a common inflammatory airway disorder characterized by reversible airflow obstruction, airway hyperresponsiveness, and airway remodeling. Although hospitalizations and mortality of asthma keep decreasing, asthma still imposes an unacceptable burden on the health care system and society.¹ Increasing studies demonstrate that asthma is heterogeneous and

has distinct phenotypes. Thus, understanding those phenotypes can lead to more targeted and personalized approaches to asthma therapy.^{2,3}

With the development of high-resolution computed tomography (HRCT), the utilization of HRCT in evaluating airway wall thickening, air trapping, emphysema, and other features has become possible. Recently, HRCT has been

Ther Adv Chronic Dis

2022, Vol. 13: 1–21

DOI: 10.1177/
20406223221084831

© The Author(s), 2022.
Article reuse guidelines:
sagepub.com/journals-
permissions

Correspondence to:

Min Xie

Department of Respiratory and Critical Care Medicine, Tongji Hospital, Tongji Medical College, Huazhong University of Science and Technology, No. 1095 Jiefang Ave., Wuhan 430030, Hubei, China

Key Laboratory of Respiratory Diseases, National Ministry of Health of the People's Republic of China and National Clinical Research Center for Respiratory Disease, Wuhan, China

xie_mr@126.com

Qiongjie Hu

Department of Radiology, Tongji Hospital, Tongji Medical College, Huazhong University of Science and Technology, No. 1095, Jiefang Avenue, Wuhan 430030, Hubei, China

qjhu@outlook.com

Zhenyu Yang

Lu Qin

Chongsheng Cheng

Shengding Zhang

Xiaoyu Fang

Zhen Li

Xiansheng Liu

Department of Respiratory and Critical Care Medicine, Tongji Hospital, Tongji Medical College, Huazhong University of Science and Technology, Wuhan, China

Key Laboratory of Respiratory Diseases, National Ministry of Health of the People's Republic of China and National Clinical Research Center for Respiratory Disease, Wuhan, China

Jinhan Qiao

Yiwen Liu

Liming Xia

Department of Radiology, Tongji Hospital, Tongji Medical College, Huazhong University of Science and Technology, Wuhan, Hubei, China

Harald Renz

Institute of Laboratory
Medicine and
Pathobiochemistry,
Molecular Diagnostics,
Philipps University
Marburg University
Hospital Giessen and
Marburg GmbH, Marburg,
Germany

Sechenov First Moscow
State Medical University,
Moscow, Russia

*Zhenyu Yang and Lu Qin
contributed equally as
co-first authors.

adopted as an effective tool to assess the clinical features of asthma patients. Previous research showed that quantitative thoracic CT-derived airway morphometry was strongly associated with epithelial thickness, airway muscle content, and lung function in asthma.⁴⁻⁷ Moreover, a sizable severe asthma cohort study⁸ indicated that 80% of asthma patients had HRCT scan abnormalities, including bronchial wall thickening, bronchiectasis, and emphysema. Inoue *et al.*⁹ have demonstrated that airway remodeling was related to CT assessments of airway involvement in patients with eosinophilic asthma. Besides, mucus plugs could contribute to chronic airflow obstruction and be linked to type 2 (T2) inflammation in chronic severe asthma patients.^{10,11} In a recent study, the values of FEV1% predicted in asthma patients with bronchiectasis were worse than those without bronchiectasis ($68.9 \pm 20.2\%$ versus $78.2 \pm 25.2\%$, $p = 0.028$).¹² As a noninvasive auxiliary examination, HRCT can serve as a promising method to estimate small and proximal airway morphometry, mucus plugs, bronchiectasis, and emphysema of asthma. However, to the best of our knowledge, the imaging features and the association with clinical characteristics and therapeutic response of untreated early-stage asthma patients have not been systemically investigated using HRCT scans.

In this study, imaging features were detected by HRCT in naïve asthma patients, defined as not receiving corticosteroids or other asthma medications for at least 1 month, and the correlation between imaging features and clinical characteristics, including the therapeutic response, were evaluated. Cluster analysis of imaging indices was then conducted to explore novel imaging phenotypes. This study may provide insights into the underlying pulmonary structure abnormalities and lead to personalized therapy strategies for naïve asthma patients.

Materials and methods

Subjects

In this study, all asthma patients ($n = 109$) and controls ($n = 50$) were consecutively recruited from April 2015 to September 2018 at the Outpatient Department of Respiratory and Critical Care Medicine, Tongji Hospital, Huazhong University of Science and Technology, China. The Ethics Review Board of Tongji Hospital approved this

study (IRB ID: 20150406), and all participants provided written informed consent prior to clinical data and sample collection. The inclusion criteria of naïve asthma patients included: (1) asthma has been diagnosed for at least 3 months according to the global initiative for asthma (GINA) 2014 guideline;¹³ (2) patients were older than 18; (3) patients have not received any corticosteroids or other asthma medications in the last month. Exclusion criteria included: (1) cancer; (2) pregnancy; (3) acute respiratory infection includes the infections of the nasal cavity, paranasal sinuses, larynx, pharynx, epiglottis, trachea, bronchioles, and lungs with duration ≤ 30 days; (4) bronchiectasis disease (with chronic productive cough and unexplained hemoptysis);¹⁴ (5) a previous diagnosis of chronic obstructive pulmonary disease (COPD);¹⁵ (6) other pulmonary diseases which the investigators considered inappropriate for this study such as interstitial lung disease and tuberculosis; (7) severe organ failures such as myocardial ischemia, acute kidney injury, respiratory failure, intestinal dysfunction, and hepatic impairment.

Healthy controls were recruited from the population who had annual routine medical examinations in Tongji Hospital. Routine physical examinations include clinical histories, physical examinations, regular pulmonary function tests, and chest CT scans. The healthy control subjects were provided with an option of CT scan as part of a routine physical examination in the annual physical examination to increase early-stage lung cancer detection. The inclusion criteria of healthy controls included: (1) age greater than 18 years; (2) who had normal results of a peripheral blood test; (3) without respiratory diseases and severe other organ diseases; (4) without atopy history; (5) without a family history of asthma or atopy. Besides, the control group did include smoking subjects.

All asthma patients' clinical characteristics and imaging indices were collected at the first visit (V1). All patients were treated for 3 months according to the GINA 2014 guideline. Finally, 75 asthma patients were followed-up and recorded with clinical improvement at the end of the 3 months [second visit (V2)] (Figure S1).

Classification of T2 inflammation phenotypes

Asthma is divided into 'T2-high' or 'T2-low' phenotypes according to the level of T2 inflammation. The measured biomarkers of T2 inflammation

included the percentage of induced sputum eosinophils, peripheral blood eosinophil count, and the fraction of exhaled nitric oxide (FeNO) concentration. High levels of the biomarkers were defined as follows: percentage of sputum eosinophils $\geq 3\%$, peripheral blood eosinophil count $\geq 300/\mu\text{l}$, and FeNO ≥ 25 ppb. Elevation in two or more biomarkers was defined as T2-high phenotype; otherwise, it was T2-low phenotype.¹⁶ Eighty-eight out of 109 patients with available data were classified into different T2 phenotypes based on the classification mentioned above criteria.

CT scanning and data acquisition

All patients underwent noncontrast CT scanning (GE Healthcare, USA; Philips, Netherlands; or Toshiba Medical Systems, Japan) of the thorax. Image equipment parameters included tube voltage 80–120 kV, automated tube current modulation, and mA ranges from 60 to 300. All data sets were reconstructed with both 60% adaptive statistical iterative reconstruction (ASIR) with a slice thickness and interval of 1.25 mm. A standard sharp lung kernel (B70f) was used in image reconstruction. All the subjects were briefly trained, and chest CT scans were performed after a full inhalation to total lung capacity (TLC).

IntelliSpace Portal (version 7.0.4, clinical application CT COPD, Philips) was performed to obtain quantitative computed tomography (QCT) parameters of airway remodeling and emphysema. Three radiologists reviewed the parameters of image bronchiectasis and mucus plugs with 6, 5, and 11 years of clinical experience, respectively, who were unaware of patient outcomes. Disagreements were resolved by consensus.

We used some previously reported HRCT-based parameters,^{7,10,17–19} including airway remodeling, emphysema, image bronchiectasis, and mucus plugs, to evaluate the imaging features of naïve asthma patients.

Airway remodeling. Airway parameters for each segment were quantified at each centerline voxel and averaged over the segmental bronchus. The third-generation airway wall measurements for all automatically segmented and labeled were averaged in each subject. We calculated the average of 18 third-generation airways per subject (10 for the right lung and 8 for the left lung). The airway

parameters including mean airway total area (TA)/body surface area (BSA), mean airway outer diameter (OD)/BSA, mean airway lumen diameter (LD)/BSA, mean airway lumen area (LA)/BSA, LA percentage (LA%), mean airway wall area (WA), WA percentage (WA%), mean airway wall thickness (WT), WT percentage (WT%) were obtained.¹⁷

Emphysema. As previously described by Xie *et al.*,¹⁹ emphysema was quantified by the percentage of low attenuation area below -950 Hounsfield units (%LAA-950) on the inspiratory images. The emphysema parameters consisted of TLC, %LAA-950, and low attenuation area below -950 HU (LAA-950) in five regions [right upper lobe (RUL), right middle lobe (RML), right lower lobe (RLL), left upper lobe (LUL), and left lower lobe (LLL)].

Bronchiectasis. The presence of bronchiectasis by the CT finding was defined when one or more of the criteria were fulfilled:¹⁸ lack of tapering of the bronchial lumen toward the periphery; the internal diameter of the bronchi was greater than that of the accompanying pulmonary artery; the presence of peripheral bronchi within 1 cm of the pleura. The ‘bronchiectasis’ in this study is the ‘image bronchiectasis’, but not the bronchiectasis disease. The extent score of bronchiectasis was calculated according to the number of affected segments. The severity of bronchiectasis was classified by 0 (no abnormality), 1 (partial noncontinuous bronchiectasis), 2 (diffusion continuous bronchiectasis), or 3 (diffusion continuous lesions that extended to the subpleural area).⁷ The distribution types of bronchiectasis were classified into the central type (only involved between 1th and 4th generations), the peripheral type (only involved up to 5th and distal generations), and the mix type (both central and peripheral were involved).

Mucus plugs. Mucus plugs were defined as complete occlusion of the airway by mucus. The evaluation and grading criteria of mucus plugs used the methodology proposed by Dunican *et al.*¹⁰ Each segment was systematically examined for the presence or absence of mucus plugs and given a score of 1 or 0, respectively, yielding a sum-up mucus score ranging from 0 to 20. The mucus number was defined as the total number of mucus plugs in all airways. Furthermore, the severity of mucus plugs was defined as zero (mucus score of 0),

low (mucus scores between 0.5 and 3.5), or high (mucus scores of 4.0 or more).¹⁰

Principal component and cluster analyses

Through the methodology presented by Gupta *et al.*,²⁰ principal component and cluster analyses were performed to obtain novel imaging phenotypes of naïve asthma patients. Sixteen quantitative CT variables used for principal component analysis were as follows: mean LD/BSA, mean WT/BSA, mean WT%, mean OD/BSA, mean WA/BSA, mean WA%, mean TA/BSA, mucus score, mucus number, mucus severity, TLC, total LAA-950, total %LAA-950, extent score of bronchiectasis, the severity of bronchiectasis, and distribution type of bronchiectasis. Before performing the principal component and cluster analyses, all variables were Z-normalized. The Kaiser–Meyer–Olkin measure for sampling adequacy was 0.652. According to the Kaiser criterion (eigenvalue > 1), the analysis identified five components contributing to the data set and accounted for 91.74% of the total population variance. Component loadings of the five independent components were shown in Table S4.

Two steps were involved in statistical cluster analysis. First, the Ward method conducted hierarchical cluster analysis (using squared Euclidean distance as the interval measure), which generated a dendrogram to determine the three clusters (Figure S2). Second, K-means cluster analysis was used as the principal clustering technique, with a prespecified number of clusters ($k=3$) to determine the cluster membership of asthma patients.

Statistical analysis

Normal data were expressed as means (SDs), and non-normal data were described as medians (interquartile ranges). χ^2 and Fisher exact tests were used to compare numeration data. Student's *t* test (for normal data) and Mann–Whitney *U* test (for non-normal data) were performed to compare two groups. One-way analysis of variance (ANOVA) with the Tukey correction (for normal data) and the Kruskal–Wallis test with the Dunn intergroup comparison (for non-normal data) were used for comparisons among multiple groups. Spearman correlation coefficient was used to determine the relationship between imaging indices and clinical features.

Receiver operating characteristic (ROC) analysis was performed for prediction of forced expiratory volume in 1s (FEV₁)% predicted (V1) < 80% based on clinical characteristics and imaging indices. Statistical analysis was performed using the IBM SPSS Statistics software version 21.0 (Chicago, IL, USA), and *p* value < .05 was considered statistically significant. Principal component and cluster analyses were performed to obtain unbiased phenotypes of imaging characteristics in asthma patients.²⁰ Power Analysis and Sample Size (PASS) software version 15.0.5 was performed to measure the needed sample size of this study based on the data from previous relevant studies. The sample size analysis has been provided in supplementary materials (see Table S1 and Table S2).

Results

Demographic and clinical characteristics

Baseline demographic and clinical characteristics of naïve asthma patients ($n=109$) and healthy controls ($n=50$) were shown in Table 1. The detailed study flowchart was illustrated in Figure S1. Asthma patients had worse lung function and more eosinophils in peripheral blood compared with healthy controls. There was no significant difference in age, sex, body mass index (BMI), or smoking status between asthma patients and healthy controls.

HRCT imaging features

Among all subjects, airway remodeling indices were not available in one asthma patient and four healthy controls, and emphysema indices of one asthma patient and three healthy controls were not measured due to image loading failure.

Morphological parameters of participants assessed by HRCT were shown in Table 2. Specifically, mean LA/BSA, mean LA%, and mean LD/BSA of asthma patients were significantly decreased compared with those of healthy controls. Accordingly, the mean WA% of asthma patients was significantly greater than that of healthy controls [70.2% (64.8–72.8%) versus 60.7% (56.7–64.1%), $p<0.0001$]. Mean WT/BSA, mean WA/BSA, and mean WT% of asthma patients were higher than those of healthy controls ($p<0.05$). Some studies found that mean WA% is a critical parameter indicating the degree of airway

Table 1. Demographic and clinical characteristics of asthma patients and healthy controls.

	Asthma patients (n = 109)	Healthy controls (n = 50)	p values
Sex, female/male (n/n)	64/45	27/23	0.577
Age (years)	45.0 (32.0–51.0)	43.0 (37.0–49.3)	0.540
BMI (kg/m ²) ^a	22.9 (2.9)	23.1 (2.6)	0.591
Smoker, n (%)	27 (24.8%)	9 (18.0%)	0.344
Smoking (pack years)	0.0 (0.0–2.0)	0.0 (0.0–0.0)	0.661
Lung function (V1)			
FEV ₁ % predicted	88.1 (76.3–99.6)	110.7 (99.3–118.8)	0.000
FEV ₁ /FVC%	70.7 (64.4–77.9)	82.3 (79.5–84.8)	0.000
PEF% predicted	86.5 (72.7–97.1)	92.6 (85.6–101.2)	0.001
MEF75/25% predicted	27.4 (18.2–47.0)	90.3 (73.6–107.3)	0.000
PD20 (mg)	0.1 (0.0–0.8)	–	–
PB-eos (×10 ⁹ /L)	0.3 (0.1–0.5)	0.1 (0.5–0.1)	0.000
PB-eos%	3.8 (1.8–7.0)	1.5 (1.0–3.0)	0.000
FeNO (ppb)	41.0 (18.6–75.3)	–	–
T-IgE (IU/mL)	99.7 (41.9–218.6)	–	–
BMI, body mass index; FeNO, fraction of exhaled nitric oxide; FEV ₁ , forced expiratory volume in 1s; FVC, forced vital capacity; MEF75/25, mid-expiratory flow velocity; PB-eos, peripheral blood eosinophil; PD20, the dose of acetylcholine causing the FEV ₁ to drop by 20%; PEF, peak expiratory flow; T-IgE, total immunoglobulin E; V1, asthma patients' first visit before treatment; –, denotes without data. Data are expressed as mean (SD), median (IQR), n/n or n (%). Values of p comparing asthma patients and healthy controls are evaluated by Pearson's χ^2 test, Fisher's exact test, Student's t test or Mann-Whitney U test. ^a Data follow Gaussian distribution.			

remodeling.^{6,17,21} In this study, the normal range of WA% was defined as 59.3% to 62.4% based on the 95% confidence interval (CI) of that in healthy control subjects. Therefore, mean WA% greater than 62.4% was considered as airway remodeling.

As for indices of emphysema, there was no significant difference in TLC, total LAA-950, or total %LAA-950 between the asthma patients and controls. Interestingly, the %LAA < -950 of the LLLs in asthma patients was increased compared with that in healthy controls ($p=0.036$) (Table 2).

The scores and the numbers of mucus in asthma patients were significantly higher than those in healthy controls ($p<0.0001$). About 18.3% of asthma patients had a low level of bronchial

mucus, and 25.7% of asthma patients had a high level of mucus (Table 2).

Image bronchiectasis prevalence was significantly higher in asthma patients than healthy controls (29.4% versus 6%, $p=0.001$). There was no bronchiectasis accompanied with mucus plugs in healthy controls, while 8.3% of asthma patients had image bronchiectasis in the presence of mucus plugs ($p<0.0001$). The extent score of bronchiectasis of asthma patients was greater than healthy controls ($p<0.0001$). Similarly, the image bronchiectasis in asthma patients was more severe than that in healthy controls ($p=0.010$). There was no significant difference in the distribution types of bronchiectasis between the two groups, although 59.4% of bronchiectasis in asthma patients were peripheral type, and 100%

Table 2. Imaging indices of asthma patients and healthy controls.

	Asthma patients (<i>n</i> = 109)	Healthy controls (<i>n</i> = 50)	<i>p</i> values
Airway remodeling	<i>n</i> = 108	<i>n</i> = 46	
Mean TA/BSA (mm ² /m ²)	27.7 (24.2–33.9)	26.6 (25.2–29.0)	0.100
Mean WA/BSA (mm ² /m ²)	19.2 (16.8–21.9)	16.4 (15.3–18.2)	0.000
Mean LA/BSA (mm ² /m ²)	8.3 (6.5–11.1)	10.3 (8.8–12.0)	0.001
Mean OD/BSA (mm/m ²) ^a	4.4 (0.6)	4.4 (0.4)	0.416
Mean LD/BSA (mm/m ²) ^a	2.6 (0.5)	2.9 (0.4)	0.000
Mean WT/BSA (mm/m ²) ^a	1.0 (0.2)	0.8 (0.1)	0.000
Mean WA%	70.2 (64.8–72.8)	60.7 (56.7–64.1)	0.000
Mean LA%	29.8 (27.2–35.2)	39.3 (35.9–43.3)	0.000
Mean WT% ^a	20.7 (2.6)	17.2 (2.1)	0.000
Emphysema	<i>n</i> = 108	<i>n</i> = 47	
TLC (mL)	3804.4 (3244.4–4712.8)	4093.4 (3326.0–4778.8)	0.927
Total LAA-950 (mL)	11.1 (4.1–40.9)	9.9 (3.7–41.1)	0.342
Total %LAA-950 (%)	0.3 (0.1–0.9)	0.2 (0.1–0.8)	0.297
RUL %LAA-950 (%)	0.1 (0.0–0.4)	0.2 (0.0–0.7)	0.814
RML %LAA-950 (%)	0.5 (0.2–1.3)	0.4 (0.2–1.7)	0.474
RLL %LAA-950 (%)	0.1 (0.0–0.3)	0.1 (0.0–0.5)	0.855
LUL %LAA-950 (%)	0.5 (0.2–1.2)	0.5 (0.2–1.4)	0.553
LLL %LAA-950 (%)	0.3 (0.1–1.0)	0.2 (0.0–0.5)	0.036
Mucus plugs	<i>n</i> = 109	<i>n</i> = 50	
Mucus score	0.0 (0.0–4.0)	0.0 (0.0–0.0)	0.000
Mucus number	0.0 (0.0–7.0)	0.0 (0.0–0.0)	0.000
Mucus severity, <i>n</i> (%)			
Zero	61 (56.0%)	50 (100.0%)	0.000
Low	20 (18.3%)	0 (0.0%)	
High	28 (25.7%)	0 (0.0%)	
Image bronchiectasis	<i>n</i> = 109	<i>n</i> = 50	
Bronchiectasis prevalence, <i>n</i> (%)	32 (29.4%)	3 (6.0%)	0.001
Upper lobes, <i>n</i> (%)	19 (17.4%)	0 (0.0%)	0.002
Middle lobes, <i>n</i> (%)	15 (13.8%)	2 (4.0%)	0.064

(Continued)

Table 2. (Continued)

	Asthma patients (<i>n</i> = 109)	Healthy controls (<i>n</i> = 50)	<i>p</i> values
Lower lobes, <i>n</i> (%)	18 (16.5%)	1 (2.0%)	0.009
Extent score of bronchiectasis	0.0 (0.0–1.0)	0.0 (0.0–0.0)	0.000
Bronchiectasis with mucus, <i>n</i> (%)	9 (8.3%)	0 (0.0%)	0.000
Severity of bronchiectasis, <i>n</i> (%)			
0	77 (70.6%)	47 (94.0%)	0.010
1	22 (20.2%)	3 (6.0%)	
2	8 (7.3%)	0 (0.0%)	
3	2 (1.8%)	0 (0.0%)	
Distribution type of bronchiectasis, <i>n</i> (%)			
Central	1 (3.1%)	0 (0.0%)	0.576
Peripheral	19 (59.4%)	3 (100.0%)	
Mix	12 (37.5%)	0 (0.0%)	

BSA, body surface area; LA, lumen area; LAA-950, low attenuation area below -950 HU; %LAA-950, the percentage of low attenuation area below -950 HU; LD, lumen diameter; LLL, left lower lobe; LUL, left upper lobe; OD, outer diameter; RLL, right lower lobe; RML, right middle lobe; RUL, right upper lobe; TA, total area; TLC, total lung capacity; WA, wall area; WT, wall thickness.

Data are expressed as mean (SD), median (IQR), or *n* (%). Values of *p* comparing asthma patients and healthy controls are evaluated by Pearson's χ^2 test, Fisher's exact test, Student's *t* test, or Mann-Whitney *U* test. The mucus number defined as the total number of mucus plugs in all airways. With respect to the severity of bronchiectasis, 0 denotes no abnormality, 1 denotes partial noncontinuous bronchiectasis, 2 denotes diffusion continuous bronchiectasis, 3 denotes diffusion continuous lesions that extended to the subpleural area. As for distribution types of bronchiectasis, central bronchiectasis means only involved between first and fourth generations, peripheral bronchiectasis means only involved up to fifth and distal generations, and mix bronchiectasis means involved both central and peripheral.

^aData follow Gaussian distribution.

of that in healthy controls were peripheral type (Table 2).

Bronchiectasis tended to be more frequent in asthma patients with a high level of mucus score than that in asthma patients with a low or zero level of mucus score (Figure 1(a)–(c)). What's more, the percentage of smoking subjects and the pack years of smoking history of asthma patients with bronchiectasis comorbid mucus plugs were greater compared with those of asthma patients without bronchiectasis ($p < 0.05$) (Figure 1(d) and (e)).

Correlation between clinical characteristics and CT imaging indices of asthma patients

The course of asthma was closely related with mean WA% ($r = 0.333, p < 0.005$), while BMI was slightly related with mean WA% ($r = 0.191, p < 0.05$). Mean WA% was inversely correlated with baseline

FEV₁% predicted and MEF75/25% predicted ($r = -0.202, p < 0.05$ and $r = -0.487, p < 0.005$, respectively). Total %LAA-950 was negatively correlated with baseline FEV₁% predicted and baseline FEV₁/forced vital capacity (FVC)% ($r = -0.340, p < 0.005$ and $r = -0.360, p < 0.005$, respectively). Mucus number was negatively correlated with baseline peak expiratory flow (PEF)% predicted and the dose of acetylcholine causing the FEV₁ to drop by 20% (PD20) ($r = -0.416, p < 0.005$; $r = -0.277, p < 0.05$; respectively). The extent score of bronchiectasis was positively correlated with smoking history ($r = 0.341, p < 0.005$) but negatively correlated with baseline FEV₁/FVC% ($r = -0.201, p < 0.05$) (Table S3).

The improvement of lung function indices, including the value of Δ FEV₁ and Δ FEV₁% predicted, was positively correlated with the CT mucus score of asthma patients (Figure 2(a) and (b), Table S4);

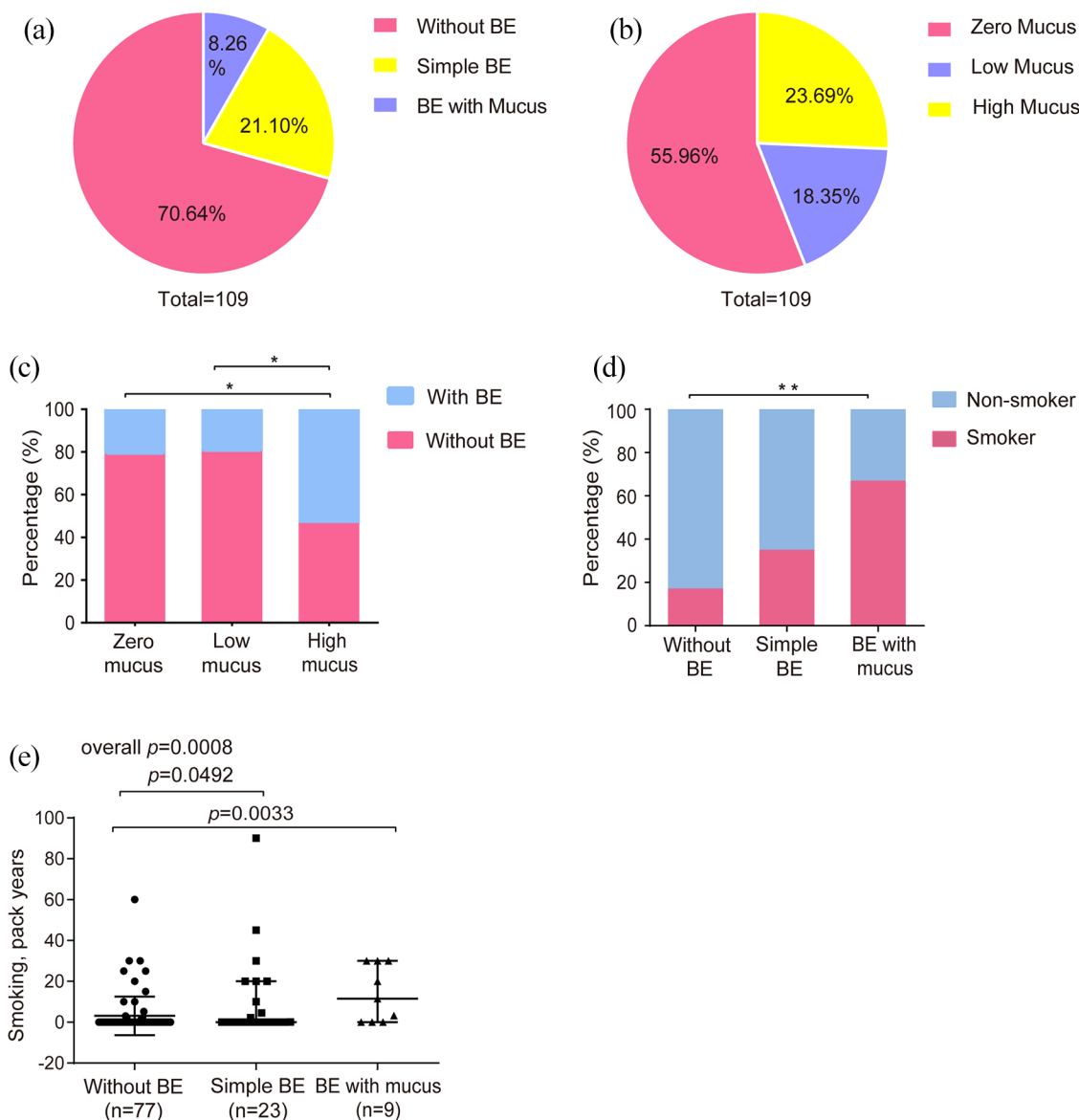


Figure 1. The relationship between image bronchiectasis and mucus plugs, smoking status in naïve asthma patients. (a) Proportions of asthma patients without bronchiectasis (without BE), simple bronchiectasis (simple BE), and bronchiectasis with mucus (BE with mucus). (b) Proportions of asthma patients classified by mucus severity. (c) Percentage of bronchiectasis in asthma patients grouped by mucus severity, * $p < 0.05$. (d) Percentage of smoking subjects in asthma patients grouped by bronchiectasis with mucus, ** $p < 0.005$. (e) Pack years of smoking are associated with bronchiectasis in asthma patients.

similarly, CT mucus score was also positively correlated with the change of asthma control test score after treatment (Δ ACT) and Δ ACT% in asthma patients (Figure 2(c) and (d), Table S4). PEF% predicted (V2) and MEF75/25% predicted (V2) were negatively correlated with mean WA% (Figure 2(e) and (f), Table S5). Besides, the extent score of bronchiectasis showed a negative correlation with the FEV₁% predicted (V2) (Figure 2(g), Table S5).

HRCT imaging indices were related to the T2 phenotype of asthma

Enrolled asthma patients were classified into T2-low ($n = 44$) and T2-high ($n = 44$) subgroups according to the expression of T2 inflammation (Table 3). The scores and the number of mucus plugs in T2-high asthma patients were significantly higher than those in T2-low asthma patients ($p < 0.0001$) (Figure 3(a) and (b), Table 3). The eosinophils in peripheral blood,

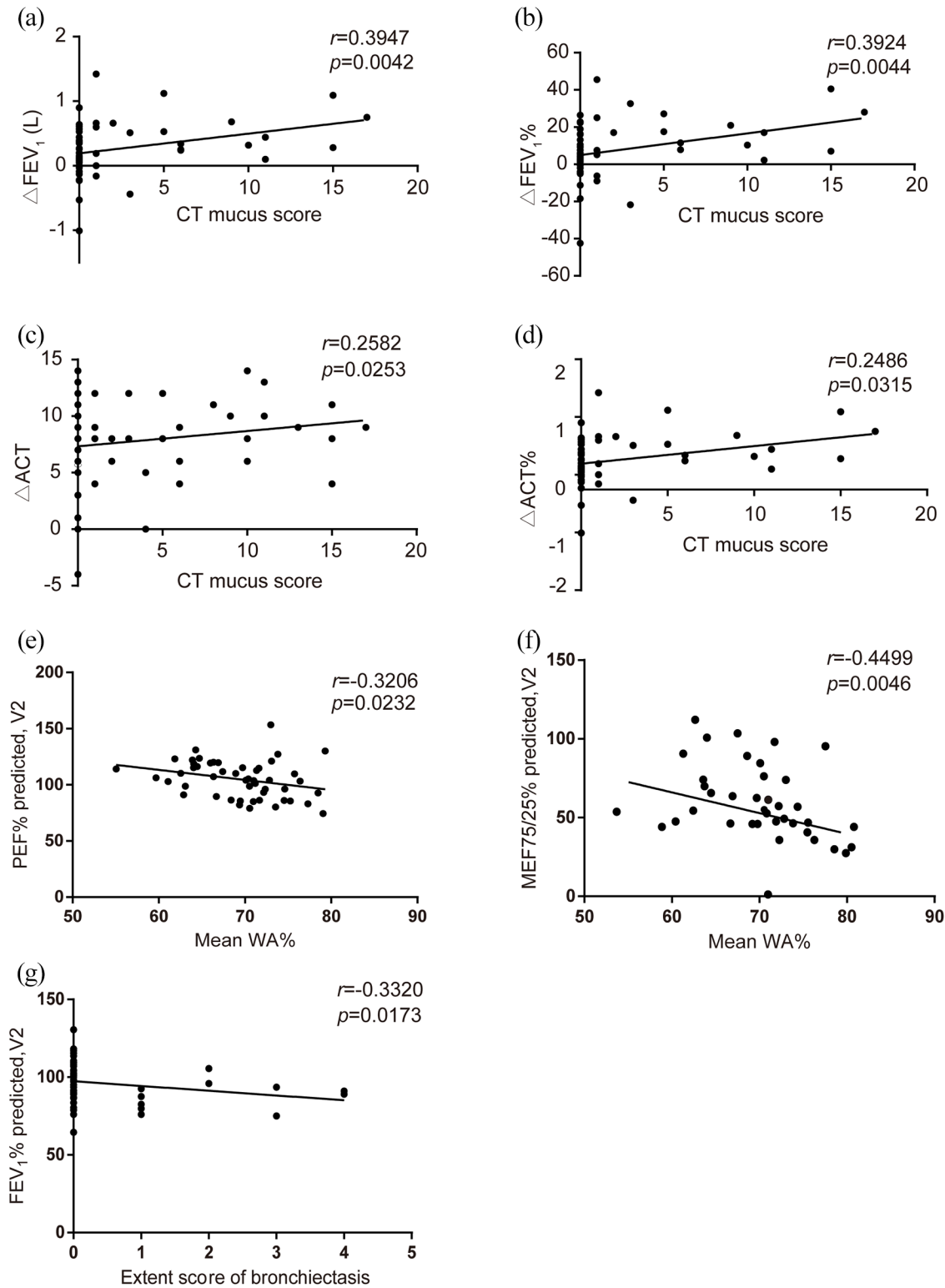


Figure 2. Correlation between imaging indices and therapeutic responsiveness. ΔFEV_1 (a), $\Delta FEV_1\%$ (b), ΔACT (c), and $\Delta ACT\%$ (d) are positively correlated with CT mucus score; contrarily, PEF% predicted (V2) (e) and MEF75/25% predicted (V2) (f) are negatively correlated with mean WA%; FEV₁% predicted (V2) (g) is negatively correlated with extent score of bronchiectasis.

Table 3. Clinical characteristics and imaging indices of asthma patients grouped by T2 inflammation.

	T2-low (n = 44)	T2-high (n = 44)	p values
Sex, female/male (n/n)	28/16	23/21	0.280
Age (years)	46.0 (40.3–50.8)	44.0 (27.3–50.5)	0.191
Onset age (years)	40.3 (29.3–47.0)	36.3 (24.2–50.5)	0.452
Course of asthma (years)	2.0 (0.5–8.0)	1.8 (0.4–6.5)	0.697
BMI (kg/m ²) ^a	22.9 (2.9)	22.6 (2.8)	0.579
Smoker, n (%)	12 (27.3%)	10 (22.7%)	0.623
Smoking (pack years)	0.0 (0.0–5.1)	0.0 (0.0–1.3)	0.444
Atopy history, n (%)	13 (29.6%)	19 (43.2%)	0.184
ACT score (V1) ^a	16.7 (3.1)	15.8 (2.6)	0.144
ACT score (V2)	24.0 (23.0–25.0)	24.0 (24.0–25.0)	0.472
Δ ACT score	7.0 (5.0–9.0)	8.0 (6.8–11.0)	0.157
Δ ACT% ^a	0.5 (0.3)	0.6 (0.3)	0.245
Lung function (V1)	n = 44	n = 43	
FEV ₁ % predicted	91.0 (84.1–100.9)	85.4 (71.5–98.4)	0.096
FEV ₁ /FVC%	72.3 (65.8–79.3)	70.8 (61.4–75.5)	0.255
PEF% predicted	88.9 (79.8–96.9)	82.7 (69.1–101.3)	0.281
MEF75/25% predicted	42.2 (29.3–62.9)	49.1 (28.0–58.2)	0.830
PD20 (mg)	0.5 (0.1–1.3)	0.0 (0.0–0.1)	0.000
Lung function (V2)	n = 19	n = 22	
FEV ₁ (L)	2.8 (2.3–3.4)	2.9 (2.2–3.4)	0.906
FEV ₁ % predicted	101.9 (89.0–109.2)	92.1 (88.7–98.8)	0.089
The change of lung function	n = 19	n = 22	
ΔFEV ₁ (L)	0.1 (0.0–0.4)	0.3 (0.1–0.7)	0.170
ΔFEV ₁ % predicted	6.0 (1.2–16.1)	8.2 (1.3–22.5)	0.619
FeNO (ppb)	18.8 (12.0–31.3)	67.0 (44.5–135.0)	0.000
T-IgE (IU/mL)	50.9 (18.7–148.2)	123.4 (74.9–359.5)	0.001
S-eos%	0.2 (0.0–1.4)	14.2 (5.6–26.3)	0.000
PB-eos (×10 ⁹ /L)	0.1 (0.1–0.2)	0.5 (0.4–0.8)	0.000
PB-eos%	1.8 (0.9–2.8)	7.3 (5.2–10.1)	0.000
Airway remodeling	n = 43	n = 44	

(Continued)

Table 3. (Continued)

	T2-low (n = 44)	T2-high (n = 44)	p values
Mean TA/BSA (mm ² /m ²)	26.5 [22.8–34.2]	28.1 [25.7–32.7]	0.161
Mean WA/BSA (mm ² /m ²) ^a	18.7 [3.8]	19.9 [4.1]	0.150
Mean LA/BSA (mm ² /m ²)	8.1 [6.4–12.0]	8.9 [7.5–10.4]	0.530
Mean OD/BSA (mm/m ²) ^a	4.4 [0.6]	4.5 [0.6]	0.356
Mean LD/BSA (mm/m ²) ^a	2.6 [0.5]	2.6 [0.4]	0.849
Mean WT/BSA (mm/m ²) ^a	1.0 [0.1]	1.0 [0.2]	0.166
Mean WA% ^a	68.2 [6.2]	69.2 [5.1]	0.425
Mean LA% ^a	31.8 [6.2]	30.9 [5.1]	0.425
Mean WT% ^a	20.3 [2.8]	20.7 [2.4]	0.477
Emphysema	<i>n</i> = 43	<i>n</i> = 44	
TLC (mL)	3690.2 [3160.4–4363.5]	3950.5 [3495.5–4981.6]	0.185
Total LAA-950 (mL)	8.9 [3.8–24.4]	14.8 [3.9–47.1]	0.218
Total %LAA-950 (%)	0.3 [0.1–0.5]	0.4 [0.1–1.1]	0.197
RUL %LAA-950 (%)	0.1 [0.0–0.4]	0.2 [0.1–0.4]	0.122
RML %LAA-950 (%)	0.4 [0.2–0.8]	0.6 [0.2–1.7]	0.215
RLL %LAA-950 (%)	0.1 [0.0–0.3]	0.1 [0.0–0.4]	0.184
LUL %LAA-950 (%)	0.4 [0.2–0.6]	0.6 [0.2–1.4]	0.296
LLL %LAA-950 (%)	0.2 [0.0–0.5]	0.4 [0.1–1.3]	0.075
Mucus plugs	<i>n</i> = 44	<i>n</i> = 44	
Mucus score	0.0 [0.0–1.0]	1.0 [0.0–9.8]	0.000
Mucus number	0.0 [0.0–1.0]	2.0 [0.0–13.0]	0.000
Mucus severity, <i>n</i> (%)			
Zero	31 (70.5%)	19 (43.2%)	0.001
Low	10 (22.7%)	8 (18.2%)	
High	3 (6.8%)	17 (18.6%)	
Image bronchiectasis	<i>n</i> = 44	<i>n</i> = 44	
Bronchiectasis prevalence, <i>n</i> (%)	12 (27.3%)	13 (29.6%)	0.813
Upper lobes, <i>n</i> (%)	6 (13.6%)	8 (18.2%)	0.560
Middle lobes, <i>n</i> (%)	5 (11.4%)	7 (15.9%)	0.534
Lower lobes, <i>n</i> (%)	9 (20.5%)	6 (13.6%)	0.395

(Continued)

Table 3. (Continued)

	T2-low (n = 44)	T2-high (n = 44)	p values
Extent score of bronchiectasis	0.0 (0.0–1.0)	0.0 (0.0–1.0)	0.769
Bronchiectasis with mucus, n (%)	2 (4.6%)	6 (13.6%)	0.266
Severity of bronchiectasis, n (%)			
0	32 (72.7%)	31 (70.5%)	0.629
1	7 (15.9%)	9 (20.5%)	
2	3 (6.8%)	4 (9.1%)	
3	2 (4.6%)	0 (0.0%)	
Distribution type of bronchiectasis, n (%)			
Central	0 (0.0%)	0 (0.0%)	0.238
Peripheral	5 (41.7%)	9 (69.3%)	
Mix	7 (58.4%)	4 (30.8%)	

BMI, body mass index; BSA, body surface area; FEV₁, forced expiratory volume in 1s; FVC, forced vital capacity; LA, lumen area; LAA-950, low attenuation area below -950 HU; %LAA-950, the percentage of low attenuation area below -950 HU; LD, lumen diameter; LLL, left lower lobe; LUL, left upper lobe; MEF75/25, mid-expiratory flow velocity; OD, outer diameter; PB-eos, peripheral blood eosinophil; PD20, the dose of acetylcholine causing the FEV₁ to drop by 20%; RML, right middle lobe; RLL, right lower lobe; RUL, right upper lobe; TA, total area; TLC, total lung capacity; WA, wall area; WT, wall thickness.

Data are expressed as mean (SD), median (IQR), n/n or n (%).

Values of *p* comparing T2-low and T2-high asthma patients are evaluated by Pearson's χ^2 test, Fisher's exact test, Student's *t* test or Mann-Whitney *U* test. Allergen skin prick testing was used to define atopy history.

^aData follow Gaussian distribution.

percentage of sputum eosinophils, and FeNO in asthma patients with high mucus scores were significantly increased compared with those in asthma patients with zero mucus score (Figure 3(c)–(e)). The serum immunoglobulin E (IgE) levels did not differ among the groups with various mucus severity (Figure 3(f)). However, the indices of airway remodeling, image bronchiectasis, and emphysema of T2-high and T2-low asthma patients were similar (Table 3).

Unbiased CT phenotyping based on cluster analysis

Sixteen CT parameters that were extracted from airway remodeling, image bronchiectasis, emphysema, and mucus indices were inputted in principal component analysis, and five components were obtained (Table S6). According to the dendrogram (Figure S2), three clusters were identified with distinct features: (1) cluster 1 had a high proportion of emphysema, moderate airway

remodeling, and moderate bronchiectasis with mild mucus plugs; (2) cluster 2 had severe airway remodeling and moderate mucus plugs with a low proportion of emphysema and mild bronchiectasis; (3) cluster 3 had severe airway remodeling, severe mucus plugs, and severe bronchiectasis with a moderate proportion of emphysema (Table 4). The severity of emphysema, airway remodeling, and bronchiectasis was defined according to the proportion of subjects greater than upper 95% CI in healthy control subjects of variables (mean WA%, total %LAA-950, and extent score of bronchiectasis, respectively). Among the three clusters, the cluster with the greatest proportion was defined as severe, and the cluster with the least proportion was defined as mild.

The three clusters had no significant difference in age, onset age, atopy history, baseline ACT score, or total immunoglobulin E (T-IgE). The proportion of female asthma patients in cluster 2 was significantly higher than that in clusters 1

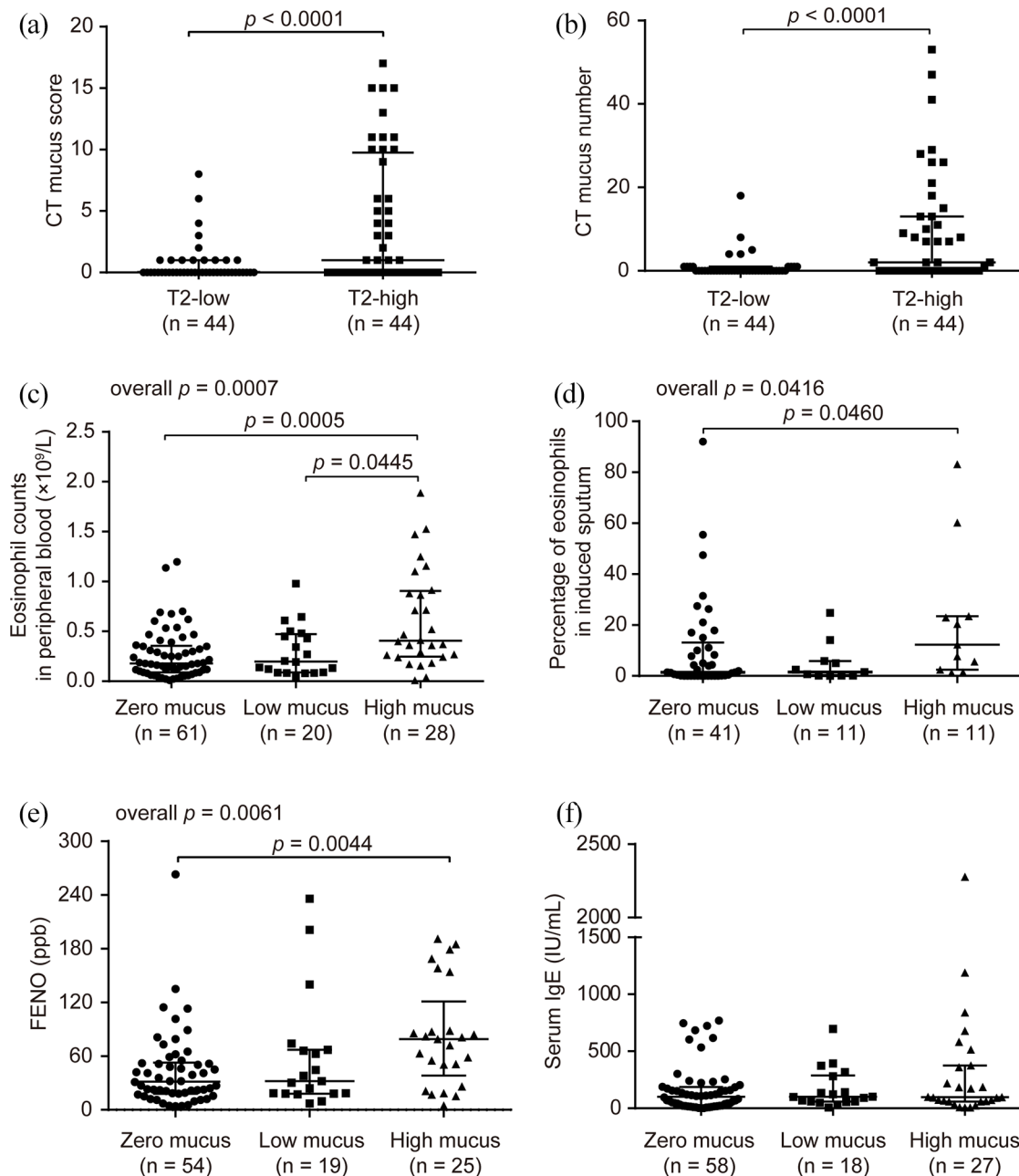


Figure 3. Relationship between T2 inflammation and CT mucus plugs in naive asthma patients. The CT mucus score (a) and CT mucus number (b) of asthma patients with T2-high phenotype are greater than those of asthma patients with T2-low phenotype. The eosinophil counts in peripheral blood (c), percentage of eosinophils in induced sputum (d), and FeNO levels (e) are associated with the severity of CT mucus in asthma patients; the serum IgE levels (f), however, do not differ from different groups classified by CT mucus (the mucus number is defined as the total number of mucus plugs in all airways).

and 3 (overall $p = 0.002$). The course of asthma in cluster 2 was significantly higher than that in cluster 1 ($p < 0.05$). Meanwhile, the BMI of asthma patients in cluster 2 was significantly higher than that in cluster 1 ($p < 0.05$). The

percentage of smokers in cluster 3 was significantly higher than that in cluster 2 ($p < 0.05$). The baseline FEV₁% predicted of cluster 3 was significantly lower than that of clusters 1 and 2 (overall $p < 0.0001$). The baseline MEF75/25%

Table 4. Quantitative CT indices of imaging phenotypes in asthma patients.

	Cluster 1: high proportion of emphysema, moderate airway remodeling and moderate bronchiectasis with mild mucus plugs (n = 34)	Cluster 2: severe airway remodeling and moderate mucus plugs with low proportion of emphysema and mild bronchiectasis (n = 55)	Cluster 3: severe airway remodeling, severe mucus plugs and severe bronchiectasis with moderate proportion of emphysema (n = 18)	p values
Airway remodeling				
Mean TA/BSA (mm ² /m ²)	32.2 (28.0–36.4)	24.3 (22.0–27.7)	30.1 (27.3–40.4)	0.000*\$
Mean WA/BSA (mm ² /m ²)	20.3 (18.0–22.0)	17.6 (15.5–20.3)	21.6 (18.7–28.8)	0.000*\$
Mean LA/BSA (mm ² /m ²)	12.0 (9.4–13.9)	7.1 (5.7–8.1)	9.6 (7.8–11.8)	0.000*\$
Mean OD/BSA (mm ² /m ²) ^a	4.7 (0.5)	4.1 (0.5)	4.8 (0.6)	0.000*\$
Mean LD/BSA (mm ² /m ²) ^a	3.0 (0.4)	2.3 (0.3)	2.8 (0.4)	0.000*##
Mean WT/BSA (mm ² /m ²) ^a	0.9 (0.1)	1.0 (0.1)	1.1 (0.2)	0.000*##
Mean WA% ^a	63.1 (4.0)	72.5 (3.5)	70.2 (4.2)	0.000*#
Mean WA% (% greater than upper 95% CI of healthy controls)	70.6%	100.0%	94.4%	0.000*#
Mean LA% ^a	36.9 (4.0)	27.5 (3.5)	29.9 (4.2)	0.000*\$
Mean WT% ^a	18.0 (1.6)	22.2 (1.8)	21.2 (1.9)	0.000*#
Emphysema				
TLC (mL) ^a	4635.3 (1167.2)	3327.1 (899.6)	4597.9 (1026.4)	0.000*\$
Total LAA-950 (ml)	19.6 (10.1–81.05)	5.3 (2.1–21.9)	20.6 (9.8–48.5)	0.000*\$
Total %LAA-950 (%)	0.4 (0.3–1.3)	0.2 (0.1–0.6)	0.5 (0.3–1.1)	0.001*\$
Total %LAA-950 (% greater than upper 95% CI of healthy controls)	54.2%	12.7%	38.9%	0.009*\$
RUL %LAA-950 (%)	0.2 (0.1–0.6)	0.1 (0.0–0.2)	0.3 (0.1–0.7)	0.000*\$
RML %LAA-950 (%)	0.7 (0.4–2.0)	0.3 (0.1–0.9)	0.8 (0.3–1.5)	0.001*\$
RLL %LAA-950 (%)	0.1 (0.0–0.4)	0.1 (0.0–0.2)	0.1 (0.0–0.5)	0.053
LUL %LAA-950 (%)	0.7 (0.5–1.7)	0.2 (0.1–0.5)	0.7 (0.4–1.6)	0.000*\$
LLL %LAA-950 (%)	0.4 (0.2–1.1)	0.2 (0.0–0.6)	0.7 (0.2–1.3)	0.003*\$
Mucus plugs				
Mucus score	0.0 (0.0–0.0)	0.0 (0.0–1.0)	10.5 (8.5–12.3)	0.000*##
Mucus number	0.0 (0.0–0.0)	0.0 (0.0–2.0)	19.5 (13.0–29.3)	0.000*##
Mucus severity, n (%)				
Zero	27 (79.4%)	33 (60.0%)	0 (0.0%)	0.000

(Continued)

Table 4. (Continued)

	Cluster 1: high proportion of emphysema, moderate airway remodeling and moderate bronchiectasis with mild mucus plugs (n = 34)	Cluster 2: severe airway remodeling and moderate mucus plugs with low proportion of emphysema and mild bronchiectasis (n = 55)	Cluster 3: severe airway remodeling, severe mucus plugs and severe bronchiectasis with moderate proportion of emphysema (n = 18)	p values
Low	6 (17.7%)	14 (25.5%)	0 (0.0%)	
High	1 (2.9%)	8 (14.6%)	18 (100.0%)	
Image bronchiectasis				
Bronchiectasis prevalence, n (%)	14 (41.2%)	4 (7.3%)	13 (72.2%)	0.000
Upper lobes, n (%)	7 (20.6%)	2 (3.6%)	10 (55.6%)	0.000
Middle lobes, n (%)	7 (20.6%)	1 (1.8%)	6 (33.3%)	0.001
Lower lobes, n (%)	10 (29.4%)	2 (3.6%)	5 (27.8%)	0.002
Extent score of bronchiectasis	0.0 (0.0–1.3)	0.0 (0.0–0.0)	1.5 (0.0–3.3)	0.000*#
Extent score of bronchiectasis (% greater than upper 95% CI of healthy controls)	23.5%	1.8%	50.0%	0.000*\$
Bronchiectasis with mucus, n (%)	2 (5.9%)	0 (0.0%)	6 (33.3%)	0.000
Severity of bronchiectasis, n (%)				
0	20 (58.8%)	51 (92.7%)	5 (27.8%)	0.000
1	9 (26.5%)	4 (7.3%)	8 (44.4%)	
2	3 (8.8%)	0 (0.0%)	5 (27.8%)	
3	2 (5.9%)	0 (0.0%)	0 (0.0%)	
Distribution type of bronchiectasis, n (%)				
Central	0 (0.0%)	1 (25.0%)	0 (0.0%)	0.058
Peripheral	7 (50.0%)	3 (75.0%)	8 (61.5%)	
Mix	7 (50.0%)	0 (0.0%)	5 (38.5%)	

LA, lumen area; LAA-950, low attenuation area below -950 HU; %LAA-950, the percentage of low attenuation area below -950 HU; LD, lumen diameter; LLL, left lower lobe; LUL, left upper lobe; MEF75/25, mid-expiratory flow velocity; OD, outer diameter; PB-eos, peripheral blood eosinophil; PD20, the dose of acetylcholine causing the FEV₁ to drop by 20%; RML, right middle lobe; RLL, right lower lobe; RUL, right upper lobe; TA, total area; TLC, total lung capacity; WA, wall area; WT, wall thickness.

Data are expressed as mean (SD), median (IQR), n/n or n (%). Values of *p* comparing cluster 1, cluster 2 and cluster 3 are evaluated by Pearson's χ^2 test, Fisher's exact test, Kruskal-Wallis test with the Dunn multiple comparison test, or one-way ANOVA with the Tukey test. **p* < 0.05, cluster 1 versus cluster 2; #*p* < 0.05, cluster 1 versus cluster 3; \$*p* < 0.05, cluster 2 versus cluster 3. Among the three clusters, the patients in the cluster with the greatest proportion of emphysema were defined as high proportion, while those in the cluster with the least proportion of emphysema were defined as low proportion of emphysema.

^aData follow Gaussian distribution.

predicted in cluster 1 was significantly higher than that in cluster 2 ($p < 0.05$). The value of ΔFEV_1 and $\Delta FEV_1\%$ predicted in cluster 3 was significantly higher than in cluster 1 (both $p < 0.05$). PD20 in cluster 3 was significantly lower than that in cluster 1 ($p < 0.05$). The proportion of T2-high asthma patients in cluster 3

was significantly higher than that in clusters 1 and 2 (overall $p < 0.05$). FeNO and eosinophils in peripheral blood in cluster 3 were significantly higher than those in clusters 1 and 2 (overall $p < 0.05$), and the eosinophils in induced sputum in cluster 3 were significantly higher than that in cluster 2 ($p < 0.05$) (Table 5).

Table 5. Clinical characteristics of imaging phenotypes in asthma patients.

	Cluster 1: high proportion of emphysema, moderate airway remodeling and moderate bronchiectasis with mild mucus plugs (n = 34)	Cluster 2: severe airway remodeling and moderate mucus plugs with low proportion of emphysema and mild bronchiectasis (n = 55)	Cluster 3: severe airway remodeling, severe mucus plugs and severe bronchiectasis with moderate proportion of emphysema (n = 18)	p values
Sex, female/male (n/n)	16/18	41/14	6/12	0.002*\$
Age (years)	46.0 (30.5–52.8)	46.0 (36.0–50.0)	41.5 (22.8–49.0)	0.179
Onset age (years)	41.0 (28.3–50.9)	41.0 (27.8–45.9)	33.5 (18.7–44.1)	0.102
Course of asthma (years)	1.0 (0.5–3.3)	3.0 (1.0–8.0)	4.5 (0.5–10.0)	0.033*
BMI (kg/m ²) ^a	22.0 (2.5)	23.8 (2.9)	22.2 (2.6)	0.005*
Smoker, n (%)	10 (29.4%)	9 (16.4%)	8 (44.4%)	0.047\$
Smoking (pack years)	0.0 (0.0–10.4)	0.0 (0.0–0.0)	0.0 (0.0–20.0)	0.080
Atopy history, n (%)	11 (32.4%)	19 (34.6%)	8 (44.4%)	0.671
ACT score (V1) ^a	16.8 (2.2)	16.1 (3.1)	15.1 (2.7)	0.130
ACT score (V2)	24.5 (23.8–25.0)	24.0 (23.0–25.0)	25.0 (23.5–25.0)	0.205
Δ ACT score ^a	8.0 (6.8–8.3)	8.0 (6.0–9.0)	9.0 (7.0–11.0)	0.251
Δ ACT% ^a	0.5 (0.2)	0.5 (0.3)	0.6 (0.3)	0.273
Lung function (V1)	n = 34	n = 55	n = 17	
FEV ₁ % predicted ^a	95.6 (12.8)	86.1 (19.1)	71.1 (14.9)	0.000*##\$
FEV ₁ /FVC%	72.9 (67.0–79.5)	69.9 (65.7–76.2)	63.1 (55.3–71.5)	0.015#
PEF% predicted ^a	97.0 (19.1)	83.0 (21.8)	68.7 (20.2)	0.000*##\$
MEF75/25% predicted ^a	57.1 (24.1)	37.5 (17.2)	54.6 (7.9)	0.011*
PD20 (mg)	0.3 (0.1–1.3)	0.1 (0.0–0.5)	0.0 (0.0–0.1)	0.004#
Lung function (V2)	n = 13	n = 28	n = 9	
FEV ₁ (L) ^a	3.2 (0.8)	2.7 (0.1)	2.9 (0.2)	0.216
FEV ₁ % predicted ^a	99.4 (8.0)	96.2 (14.3)	90.8 (13.7)	0.307
The change of lung function	n = 13	n = 28	n = 9	

(Continued)

Table 5. (Continued)

	Cluster 1: high proportion of emphysema, moderate airway remodeling and moderate bronchiectasis with mild mucus plugs (n = 34)	Cluster 2: severe airway remodeling and moderate mucus plugs with low proportion of emphysema and mild bronchiectasis (n = 55)	Cluster 3: severe airway remodeling, severe mucus plugs and severe bronchiectasis with moderate proportion of emphysema (n = 18)	p values
Δ FEV ₁ (L) ^a	0.1 (0.5)	0.3 (0.4)	0.6 (0.4)	0.030#
Δ FEV ₁ % predicted ^a	1.2 (16.9)	7.7 (14.3)	18.5 (12.0)	0.032#
T2 inflammation phenotypes, n (%)	n = 31	n = 42	n = 13	
T2-high asthmatics	12 (38.7%)	18 (42.9%)	13 (100.0%)	0.000
T2-low asthmatics	19 (61.3%)	24 (57.1%)	0 (0.0%)	
FeNO (ppb)	24.0 (18.3–51.1)	38.0 (15.3–66.0)	81.0 (54.9–123.4)	0.001#
T-IgE (IU/mL)	86.2 (32.2–191.0)	98.0 (47–185.7)	173.2 (82.7–547.9)	0.136
S-eos%	1.9 (0.1–14.1)	2.0 (0.0–10.1)	20.4 (5.6–60.2)	0.048\$
PB-eos ($\times 10^9$ /L)	0.2 (0.1–0.3)	0.2 (0.1–0.4)	0.6 (0.3–1.1)	0.000#
PB-eos%	2.7 (1.5–5.5)	3.3 (1.8–6.8)	8.3 (4.9–11.5)	0.000#

ACT: asthma control test; Δ ACT: The change of asthma control test score after treatment; Δ ACT % = Δ ACT/ACT (V1); Δ FEV₁: The change of forced expiratory volume in 1s after treatment; FeNO: fractional exhaled nitric oxide; S-eos: sputum eosinophil; T2: Type 2; T-IgE: total immunoglobulin E; V2: second visit.

Data are expressed as mean (SD), median (IQR), *n/n* or *n* (%). Values of *p* comparing cluster 1, cluster 2 and cluster 3 are evaluated by Pearson's χ^2 test, Fisher's exact test, Kruskal-Wallis test with the Dunn multiple comparison test, or one-way ANOVA with the Tukey test.

^aData follow Gaussian distribution. **p* < 0.05, cluster 1 versus cluster 2; #*p* < 0.05, cluster 1 versus cluster 3; \$*p* < 0.05, cluster 2 versus cluster 3.

ROC curve for predicting baseline FEV₁% predicted

ROC analysis was applied for the prediction of baseline FEV₁% predicted (Figure 4, Table S7). Eleven clinical parameters and 16 imaging indices were separately used to predict the baseline FEV₁% predicted (V1) < 80%. The results showed that only four indicators, including course of asthma, mucus number, the eosinophils in peripheral blood, and total %LAA-950, presented with an area under the curve (AUC) value of greater than 0.6 (0.657, 0.674, 0.630, and 0.649, respectively), and the AUC values of the remaining indicators were not good enough to be included in the final model. Consequently, the four parameters were together employed to predict the FEV₁% predicted (V1) < 80%, which showed improved prediction effectiveness (AUC = 0.753) (Table S7).

Discussion

The patients enrolled in this study were mainly in the early stage with relatively mild-moderate asthma, and the findings were consistent with the previous report that the abnormalities were present in the morphological structure of the airway and related to asthma severity and lung function.^{4,8} At the same time, the results in this study demonstrated that even in naïve early-stage asthma patients, both WA% and WT% were much greater than those in healthy controls. Besides, these indices of airway thickening were significantly correlated with lung function, especially PEF% and MEF75/25%, the markers of small airway function. Thus, we speculated that airway remodeling might happen in early-stage asthma and probably be more prominent in the distal airway.²²

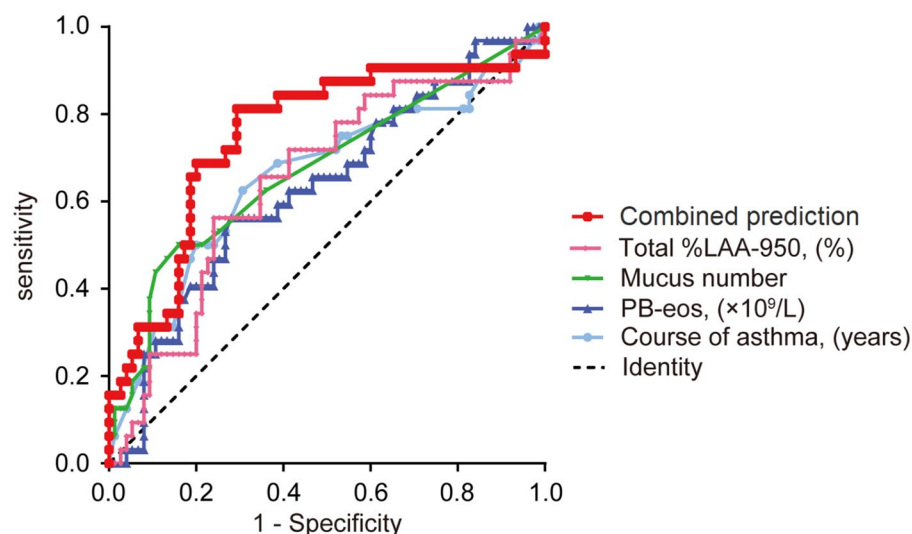


Figure 4. ROC analysis for clinical characteristics and imaging indices prediction of FEV₁% predicted (V1) < 80%. The ROC curves show the parameters of course of asthma, mucus number, the eosinophil counts in peripheral blood (PB-eos, $\times 10^9/L$), total %LAA-950, and combined prediction model in diagnosing baseline airflow limitation determined by FEV₁% predicted (V1) < 80%.

Interestingly, 6% of the healthy controls were accompanied by slightly partial noncontinuous image bronchiectasis in the chest CT scan, and only one lung segment was involved in bronchiectasis in this study. The finding of a cross-sectional, retrospective study in South Korea was similar to our study. Among the 27 617 healthy population screened, 1005 were diagnosed with asymptomatic bronchiectasis based on CT findings.²³ In a previous severe asthma cohort study, the prevalence of emphysema was around 8%.⁸ The patients in our study were mainly mild or moderate asthma patients without occupational exposure to dust or other noxious gases, which partially explained that there was almost no difference in the indices of emphysema between asthma patients and healthy controls. Besides, in our study, only 35.7% of asthma patients with emphysema were smokers. What's more, 12 healthy controls had the CT features of emphysema quantified by %LAA-950, but none were smokers. It is more likely that the healthy controls and the asthma groups contain some subjects with small airway dysfunction than under-diagnosed COPD patients.^{24,25}

The results revealed T2 inflammation was closely associated with mucus plugs rather than airway remodeling, emphysema, or image bronchiectasis in naïve asthma patients. The eosinophilic inflammation helps the development of mucus plugs,

and eosinophil peroxidase (EPO)-generated oxidants might mediate mucus plug formation.^{10,11} This study also indicated that the prevalence of image bronchiectasis was greater in asthma patients with high mucus plugs than in patients with zero or low mucus plugs. It might be related to the destructive damage of the airway structure by the T2 inflammation.¹⁰ While it must be mentioned in this study, the smoking history was much higher in the patients who coexisted with image bronchiectasis and mucus plugs compared with other patients. Meanwhile, the rate of asthma patients with a smoking history in this study is similar to other major reports about asthma.²⁶⁻²⁸ Therefore, we speculate that smoking could cooperate with T2 inflammation to aggravate mucus production and damage to the pulmonary structure.

Regarding the response of asthma therapy, the results showed that the mucus score was slightly or moderately positively correlated with improvement of both lung function (i.e. ΔFEV_1 and $\Delta FEV_1\%$) and symptoms (i.e. ΔACT and $\Delta ACT\%$), which might be due to the good correlation between mucus plugs and T2 inflammation. However, the extent score of bronchiectasis was slightly inversely correlated to post-treatment FEV₁% predicted, indicating that the asthma patients with bronchiectasis might have irreversible airway damage, resulting in poor lung

function improvement. The previous report showed that bronchiectasis could also increase exacerbation rates and lead to respiratory function impairment.²⁹

Considering that not all patients could finish lung function examination, ROC analysis integrating clinical features and imaging indices was adopted to forecast FEV₁% predicted. The results showed that the predicting model combining course of asthma, peripheral blood eosinophils, mucus number, and total %LAA-950 had higher sensitivity and specificity than the results using any single variable.

In this study, three novel imaging phenotypes were derived through cluster analysis, i.e. cluster 1 with a high proportion of emphysema, cluster 2 with severe airway remodeling, and cluster 3 with severe airway remodeling, mucus plugs, and bronchiectasis. The three imaging phenotypes exhibited distinct clinical features and therapeutic responses. Cluster 1 patients with the best lung function had the worst therapeutic responses and the lowest T2 inflammation; cluster 2 patients had the highest BMI and relatively good lung function, and they had moderate therapeutic responses and moderate T2 inflammation; as for the cluster 3 patients, they held the longest course of asthma, the greatest percentage of smokers, and the worst lung function, and they had the best therapeutic responses and highest T2 inflammation. It may be interpreted that the T2 signature in asthma is strongly linked to corticosteroids responses.^{30,31} Therefore, Cluster 1 patients with the lowest T2 inflammation had the worst therapeutic responses, cluster 2 patients with moderate T2 inflammation had the moderate therapeutic responses, and cluster 3 patients with the highest T2 inflammation had the best therapeutic responses. Previous research on imaging phenotype mainly used imaging parameters of air trapping and airway structure in cluster analysis, through which clinical characteristics were generally analyzed.^{20,32–34} In this study, parameters of airway remodeling, emphysema, mucus plugs, and image bronchiectasis were systematically considered, and three unbiased novel imaging phenotypes were proposed, which showed good consistency with both clinical characteristics and T2 inflammation. Besides, three unbiased novel imaging phenotypes were derived through cluster analysis. Each cluster has its unique clinical

characteristics, and the relationships among the three clusters were not progressive. Similar results were observed among the three clusters without a smoking history.

The findings in this study indicate asthma patients have various structure abnormalities from lung CT scans. Even in naïve asthma patients, airway remodeling exists in a certain proportion of patients. Although currently it is not common for asthma patients to have a CT scan, the findings in this study, along with many others, indicate asthma patients may benefit a lot from HRCT scan, especially for those with smoking history, those incapable of completing the qualified pulmonary function test, and those with a long course and poor condition. First of all, considering not all patients could succeed in finishing lung function examination, this study's prediction model could help predict the initial lung function and initiate appropriate therapy. Second, for asthma patients, especially with smoking history, HRCT characteristics can be used to identify the specific cluster and predict the treatment responsiveness of patients, and then would be very helpful for the individualized treatment. Finally, HRCT scans would be much helpful to identify the irreversible bronchiectasis and airway remodeling, which may probably exist in patients with a long course of asthma.

There are several potential limitations in this study. First, the patients have not conducted the HRCT examinations post-treatments, making the assessment of changes in imaging characteristics after treatment unavailable. Second, the sample number of asthma patients was limited in this cohort, and the test of periostin, IL-4, or IL-5 was not available to assess and verify T2 phenotypes. Third, the novel image phenotypes of naïve asthma patients were proposed in this single-center cohort study, and further studies with a larger size of subjects are needed to verify the findings of this study.

In conclusion, naïve asthma patients have significant HRCT features such as airway remodeling, mucus plugs, and image bronchiectasis compared with healthy controls. Based on the functional respiratory imaging features, three novel imaging phenotypes can be derived, showing good consistency with clinical characteristics, therapeutic response, and T2 inflammation.

Acknowledgements

When writing this article, we benefited from the participation of teachers and classmates. They generously helped us collect the required information and gave us many valuable suggestions.

Author contributions

Zhenyu Yang: Data curation; Formal analysis; Investigation; Methodology; Writing – original draft.

Lu Qin: Formal analysis; Writing – original draft.

Jinhan Qiao: Conceptualization; Data curation; Writing – review & editing.

Chongsheng Cheng: Formal analysis.

Yiwen Liu: Formal analysis.

Shengding Zhang: Formal analysis.

Xiaoyu Fang: Formal analysis.

Zhen Li: Formal analysis.

Harald Renz: Formal analysis; Writing – review & editing.

Xiansheng Liu: Formal analysis; Writing – review & editing.

Liming Xia: Formal analysis.

Qiongjie Hu: Conceptualization; Supervision; Writing – review & editing.

Min Xie: Conceptualization; Investigation; Methodology; Project administration; Resources; Supervision; Writing – review & editing.

Availability of data and material

All data included in this study are available from the corresponding author upon reasonable request.

Funding

The authors disclosed receipt of the following financial support for the research, authorship, and/or publication of this article: This project was supported by grants from the National Natural Science Foundation of China (81670020).

Conflict of interest statement

The authors declared no potential conflicts of interest with respect to the research, authorship, and/or publication of this article.

Ethics approval and consent to participate

Ethics approval for the study protocol was obtained from the Ethical Review Board of Tongji Hospital, Tongji Medical College, Huazhong University of Science and Technology (IRB ID: 20150406).


Consent for publication

All authors critically revised the manuscript and approved the final manuscript.

ORCID iDs

Lu Qin  <https://orcid.org/0000-0002-6006-4968>

Qiongjie Hu  <https://orcid.org/0000-0001-8910-0785>

Min Xie  <https://orcid.org/0000-0003-4052-1647>

References

1. Global Initiative for Asthma. Global strategy for asthma management and prevention, 2019 <https://ginasthma.org/> (accessed 21 August 2019).
2. Anderson GP. Endotyping asthma: new insights into key pathogenic mechanisms in a complex, heterogeneous disease. *Lancet* 2008; 372: 1107–1119.
3. Wenzel SE. Asthma phenotypes: the evolution from clinical to molecular approaches. *Nat Med* 2012; 18: 716–725.
4. Gupta S, Siddiqui S, Haldar P, *et al.* Quantitative analysis of high-resolution computed tomography scans in severe asthma subphenotypes. *Thorax* 2010; 65: 775–781.
5. Kurashima K, Hoshi T, Takayanagi N, *et al.* Airway dimensions and pulmonary function in chronic obstructive pulmonary disease and bronchial asthma. *Respirology* 2012; 17: 79–86.
6. Berair R, Hartley R, Mistry V, *et al.* Associations in asthma between quantitative computed tomography and bronchial biopsy-derived airway remodelling. *Eur Respir J* 2017; 49: 1601507.
7. Kim S, Lee CH, Jin KN, *et al.* Severe asthma phenotypes classified by site of airway involvement and remodeling via chest CT scan. *J Investig Allergol Clin Immunol* 2018; 28: 312–320.
8. Gupta S, Siddiqui S, Haldar P, *et al.* Qualitative analysis of high-resolution CT scans in severe asthma. *Chest* 2009; 136: 1521–1528.
9. Inoue H, Ito I, Niimi A, *et al.* CT-assessed large airway involvement and lung function decline in eosinophilic asthma: the association between induced sputum eosinophil differential counts and airway remodeling. *J Asthma* 2016; 53: 914–921.

10. Dunican EM, Elicker BM, Gierada DS, *et al.* Mucus plugs in patients with asthma linked to eosinophilia and airflow obstruction. *J Clin Invest* 2018; 128: 9971009.
11. Svenningsen S, Haider E, Boylan C, *et al.* CT and functional MRI to evaluate airway mucus in severe asthma. *Chest* 2019; 155: 1178–1189.
12. Zamarron E, Romero D, Fernández-Lahera J, *et al.* Should we consider paranasal and chest computed tomography in severe asthma patients. *Respir Med* 2020; 169: 106013.
13. Global Initiative for Asthma. Global strategy for asthma management and prevention, 2014 <https://ginasthma.org/> (accessed 14 October 2014).
14. Flume PA, Chalmers JD and Olivier KN. Advances in bronchiectasis: endotyping, genetics, microbiome, and disease heterogeneity. *Lancet* 2018; 392: 880–890.
15. Rabe KF and Watz H. Chronic obstructive pulmonary disease. *Lancet* 2017; 389: 1931–1940.
16. Busse WW, Holgate ST, Wenzel SW, *et al.* Biomarker profiles in asthma with high vs low airway reversibility and poor disease control. *Chest* 2015; 148: 1489–1496.
17. Aysola RS, Hoffman EA, Gierada D, *et al.* Airway remodeling measured by multidetector CT is increased in severe asthma and correlates with pathology. *Chest* 2008; 134: 1183–1191.
18. Perera P and Screaton N. Radiological features of bronchiectasis. *Bronchiectasis. European Respiratory Monograph*, 2011; 2011: 44–67.
19. Xie M, Wang W, Dou S, *et al.* Quantitative computed tomography measurements of emphysema for diagnosing asthma-chronic obstructive pulmonary disease overlap syndrome. *Int J Chron Obstruct Pulmon Dis* 2016; 11: 953–961.
20. Gupta S, Hartley R, Khan UT, *et al.* Quantitative computed tomography-derived clusters: redefining airway remodeling in asthmatic patients. *J Allergy Clin Immunol* 2014; 133: 729–738.
21. Yang MS, Choi S, Choi Y, *et al.* Association between airway parameters and abdominal fat measured via computed tomography in asthmatic patients. *Allergy Asthma Immunol Res* 2018; 10: 503–515.
22. Jiang D, Wang Z, Yu N, *et al.* Airway remodeling in asthma: evaluation in 5 consecutive bronchial generations by using high-resolution computed tomography. *Respir Care* 2018; 63: 1399–1406.
23. Kim SH, Jung YJ, Ko MS, *et al.* Prevalence of asymptomatic bronchiectasis and associations among the health screening population in South Korea. *ERJ Open Res* 2021; 7: 00188–2021.
24. Janssen R and Wouters EFM. Loss of alveolar attachments as a pathomechanistic link between small airway disease and emphysema. *Am J Respir Crit Care Med* 2020; 201: 878–879.
25. McDonough JE, Yuan R, Suzuki M, *et al.* Small-airway obstruction and emphysema in chronic obstructive pulmonary disease. *N Engl J Med* 2011; 365: 1567–1575.
26. Stapleton M, Howard-Thompson A, George C, *et al.* Smoking and asthma. *J Am Board Fam Med* 2011; 24: 313–322.
27. Huang K, Yang T, Xu J, *et al.* Prevalence, risk factors, and management of asthma in China: a national cross-sectional study. *Lancet* 2019; 394: 407–418.
28. Jaakkola JJK, Hernberg S, Lajunen TK, *et al.* Smoking and lung function among adults with newly onset asthma. *BMJ Open Respir Res* 2019; 6: e000377.
29. Crimi C, Ferri S, Campisi R, *et al.* The link between asthma and bronchiectasis: state of the art. *Respiration* 2020; 99: 463–476.
30. Chung KF. Asthma phenotyping: a necessity for improved therapeutic precision and new targeted therapies. *J Intern Med* 2016; 279: 192–204.
31. Yoshida Y, Takaku Y, Nakamoto Y, *et al.* Changes in airway diameter and mucus plugs in patients with asthma exacerbation. *PLoS ONE* 2020; 15: e0229238.
32. Hartley RA, Barker BL, Newby C, *et al.* Relationship between lung function and quantitative computed tomographic parameters of airway remodeling, air trapping, and emphysema in patients with asthma and chronic obstructive pulmonary disease: a single-center study. *J Allergy Clin Immunol* 2016; 137: 1413–1422.
33. Choi S, Hoffman EA, Wenzel SE, *et al.* Quantitative computed tomographic imaging-based clustering differentiates asthmatic subgroups with distinctive clinical phenotypes. *J Allergy Clin Immunol* 2017; 140: 690–700.
34. Zhang X, Xia T, Lai Z, *et al.* Uncontrolled asthma phenotypes defined from parameters using quantitative CT analysis. *Eur Radiol* 2019; 29: 2848–2858.